

# Analogy between the “Hidden Order” and the Orbital Antiferromagnetism in $\text{URu}_{2-x}\text{Fe}_x\text{Si}_2$

H.-H. Kung,<sup>1,\*</sup> S. Ran,<sup>2,3</sup> N. Kanchanavatee,<sup>2,3</sup> V. Krapivin,<sup>1</sup> A. Lee,<sup>1</sup>  
J. A. Mydosh,<sup>4</sup> K. Haule,<sup>1</sup> M. B. Maple,<sup>2,3</sup> and G. Blumberg<sup>1,5,†</sup>

<sup>1</sup>*Department of Physics & Astronomy, Rutgers University, Piscataway, New Jersey 08854, USA*

<sup>2</sup>*Department of Physics, University of California San Diego, La Jolla, California 92093, USA*

<sup>3</sup>*Center for Advanced Nanoscience, University of California San Diego, La Jolla, California 92093, USA*

<sup>4</sup>*Kamerlingh Onnes Laboratory, Leiden University, 2300 RA Leiden, The Netherlands*

<sup>5</sup>*National Institute of Chemical Physics and Biophysics, 12618 Tallinn, Estonia*

We study  $\text{URu}_{2-x}\text{Fe}_x\text{Si}_2$ , in which two types of staggered phases compete at low temperature as the iron concentration  $x$  is varied: the nonmagnetic “hidden order” (HO) phase below the critical concentration  $x_c$ , and unconventional antiferromagnetic (AF) phase above  $x_c$ . By using polarization resolved Raman spectroscopy, we detect a collective mode of pseudovector-like  $A_{2g}$  symmetry whose energy continuously evolves with increasing  $x$ ; it monotonically decreases in the HO phase until it vanishes at  $x = x_c$ , and then reappears with increasing energy in the AF phase. The mode’s evolution provides direct evidence for unified order parameter for both nonmagnetic and magnetic phases arising from the orbital degrees-of-freedom of the uranium-5f electrons.

$\text{URu}_2\text{Si}_2$  holds long-standing interest in the strongly correlated electron community due to several emergent types of long range orders it exhibits. Below the second order phase transition temperature  $T_{\text{DW}}(x)$ , two density-wave-like phases involving long range ordering of the uranium-5f electrons compete when a critical parameter  $x$  is tuned [1], where  $x$  can be chemical substituent concentration [2, 3], pressure [4, 5] or magnetic field [6, 7]. At  $x < x_c$ , the system settles in the enigmatic “hidden order” (HO) phase [8–10], which transforms into an unconventional large moment antiferromagnetic (LMAF) phase through a first order transition for  $x > x_c$ . Below 1.5 K, a superconducting state, which likely breaks time reversal symmetry [11], emerges from the HO phase.

Recently, much effort has been dedicated towards unraveling the order parameter of the HO phase through several newly developed experimental and theoretical techniques [11–16]. In particular, the symmetry analysis of the low temperature Raman scattering data implies that the reflection symmetries of tetragonal  $D_{4h}$  point group (No. 139  $I4/mmm$ ) associated with the paramagnetic (PM) state are broken, and that a chirality density wave emerges as the HO ground state [17].

The HO and LMAF phases are known to exhibit “adiabatic continuity” [21]; i.e., both phases possess similar electronic properties [2, 22], and the Fermi surface practically shows no change across the phase boundary [21]. Furthermore, inelastic neutron scattering observed a dispersive collective excitation in the HO phase [5, 23] and recently in the LMAF phase of pressurized  $\text{URu}_2\text{Si}_2$  [24]. This raises the intriguing question of the symmetry relation between the two phases. However, experimental progress is hindered due to inherent constraints of low temperature pressurized experiments.

The availability of  $\text{URu}_{2-x}\text{Fe}_x\text{Si}_2$  crystals [2, 3] made it possible to perform high-resolution spectroscopic experiments at low temperature and ambient pressure in

both the HO and LMAF phases. Iron substitution mimics the effect of applying small pressure or in-plane stress on the  $\text{URu}_2\text{Si}_2$  lattice, and the iron (Fe) concentration,  $x$ , can be approximately treated as an effective “chemical pressure” [2]. Recently, the phase diagram of  $\text{URu}_{2-x}\text{Fe}_x\text{Si}_2$  single crystals have been determined [1, 3, 18, 25, 26], which resembles the low pressure phase diagram of pristine  $\text{URu}_2\text{Si}_2$  [4, 16] [Fig. 1(a)]. The inelastic neutron scattering measurements again illustrate the analogies of the LMAF phase to the HO phase [26, 27], albeit differences remain relating to the existence of the resonance in the LMAF state of pressurized [24, 27] or Fe-substituted crystals [26].

In this Letter, we study the dynamical fluctuations between the competing nonmagnetic HO and the time-reversal-symmetry breaking LMAF ground states in  $\text{URu}_{2-x}\text{Fe}_x\text{Si}_2$  as a function of  $x$  using polarization resolved Raman spectroscopy [28]. Albeit the distinct discrete symmetries are broken above and below the critical concentration  $x_c$ , we detect a collective mode continuously evolving with parameter  $x$  in the pseudovector-like  $A_{2g}$  symmetry channel. In the HO phase, the mode energy decreases as  $x$  is increased, disappearing at the critical Fe concentration  $x_c$ . In the LMAF phase, the collective mode again emerges in the same  $A_{2g}$  symmetry channel with the energy increasing with  $x$ . The continuous transformation of this collective excitation, a photoinduced transition between the HO and LMAF electronic phases, provides direct experimental evidence for a unified order parameter for both nonmagnetic and magnetic phases arising from the orbital degree of freedom of the uranium-5f electrons.

The polarized Raman spectra were acquired in a quasibackscattering geometry from the  $ab$  surface of  $\text{URu}_{2-x}\text{Fe}_x\text{Si}_2$  single crystals grown by the Czochralski method [28]. We use 752.5 nm line of a  $\text{Kr}^+$  laser for excitation. The scattered light was analyzed by a cus-

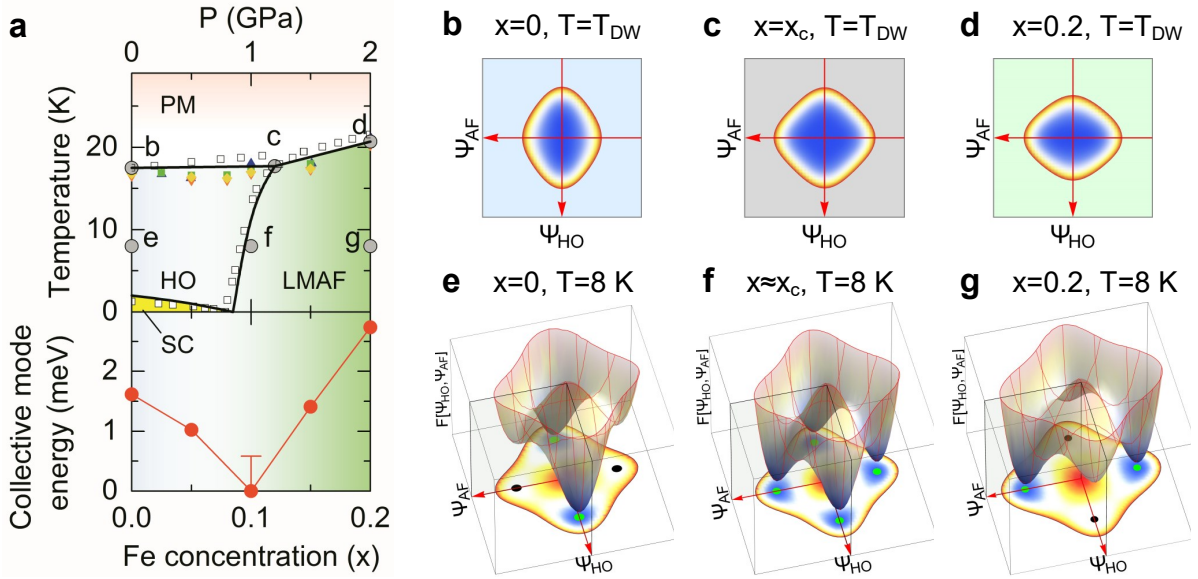


FIG. 1. (a) The upper panel shows the phase diagram of  $\text{URu}_2\text{Si}_2$  system, where the black lines show the phase boundaries. The measurements on the iron substituted  $\text{URu}_{2-x}\text{Fe}_x\text{Si}_2$  crystals from neutron diffraction [18] (blue triangle), electrical resistivity [2] (green square), magnetic susceptibility [2] (purple triangle), and heat capacity [3] (yellow diamond), are overlaid with the neutron diffraction results for  $\text{URu}_2\text{Si}_2$  under hydrostatic pressure [4] (open square) to show the similarity between the two tuning parameters. The lower panel shows the dependence of the  $A_{2g}$  collective mode energy on the Fe concentration,  $x$  [Fig. 2]. At the critical concentration,  $x = 0.1$ , the mode maximum is below the accessible energy cutoff. Therefore, the data point is placed at zero energy, with the error bar reflecting the instrumental cutoff. (b)–(g) Schematics of the Ginzburg-Landau free energy in Eq. (1) at various special points in the phase diagram [solid gray circles in (a)].  $\psi_{HO}$  and  $\psi_{AF}$  are the real and imaginary part of the hexadecapole order parameter, respectively [19, 20].

tom triple-grating spectrometer. The laser spot size on the sample is roughly  $50 \times 100 \mu\text{m}^2$ . The power on the sample is about 12 mW for most temperatures, and kept below 6 mW to achieve the lowest temperatures.

Figure 2 shows the temperature dependence of the Raman response in the eminent  $A_{2g}$  symmetry channel of the  $D_{4h}$  group, which transforms as a pseudovector [29]. The upper panels show the intensity plots of the low energy Raman response  $\chi''_{A_{2g}}(\omega, T)$  below 30 K. Above  $T_{DW}(x)$ , a quasielastic peak (QEP) comprises most of the spectral weight for all samples, narrowing towards the transition. The observed QEP originates from overdamped excitations between quasidegenerate crystal field states [17, 19], and the narrowing of the QEP with cooling is due to the increase of excitation lifetime, related to the development of a hybridization gap and formation of a heavy Fermi liquid [30, 31].

Below  $T_{DW}(x)$ , the most significant feature in the  $A_{2g}$  channel is a sharp collective mode. The sharpness of this resonance suggests the lack of relaxation channels due to the opening of an energy gap [1, 30, 32]. In order to see the mode's lineshape more clearly, we plot  $\chi''_{A_{2g}}(\omega, T)$  for each Fe concentration  $x$  in the lower panels, with  $T \approx T_{DW}(x)/2$ . The lineshapes broaden with increasing  $x$  owing to the inhomogeneity of the local stress field, or unsuppressed relaxation channels introduced by doping that interact with the collective mode, which may also be

related to the increasing continuum in the  $x = 0.15$  and  $0.2$  spectra. In contrast to the monotonic broadening of the lineshape width, the collective mode frequency shows nonmonotonic behavior as function of  $x$ . The mode energy versus Fe concentration  $x$  is shown in the lower panel of Fig. 1(a). The energy decreases with increasing  $x$  in the HO phase, until it vanishes below the instrumental resolution at  $x = 0.10$ , which is close to the HO and LMAF phase boundary determined by elastic neutron scattering [18] and thermal expansion measurements [3]. The resonance reappears in the LMAF phase, where the energy increases with increasing  $x$ . The resonance in the LMAF state appears in the same  $A_{2g}$  symmetry channel as the collective mode in the HO phase.

The similarity of the Raman response in the HO and LMAF phases encourages us to compare our results with the magnetic susceptibility. Figure 3 shows the temperature dependence of the real part of the static  $A_{2g}$  Raman susceptibility  $\chi_{A_{2g}}(0, T)$ , compared with the  $c$  axis magnetic susceptibility  $\chi_c^m(T)$  [3]. While there are discrepancies around the maxima at about 50–100 K, both quantities follow the same Curie-Weiss-like temperature dependence above 100 K, followed by a suppression approaching the second order phase transition.

The comparison between  $\chi_{A_{2g}}(0, T)$  and  $\chi_c^m(T)$  has been studied within the frame work of a phenomenological minimal model [17, 19]. The model is composed of

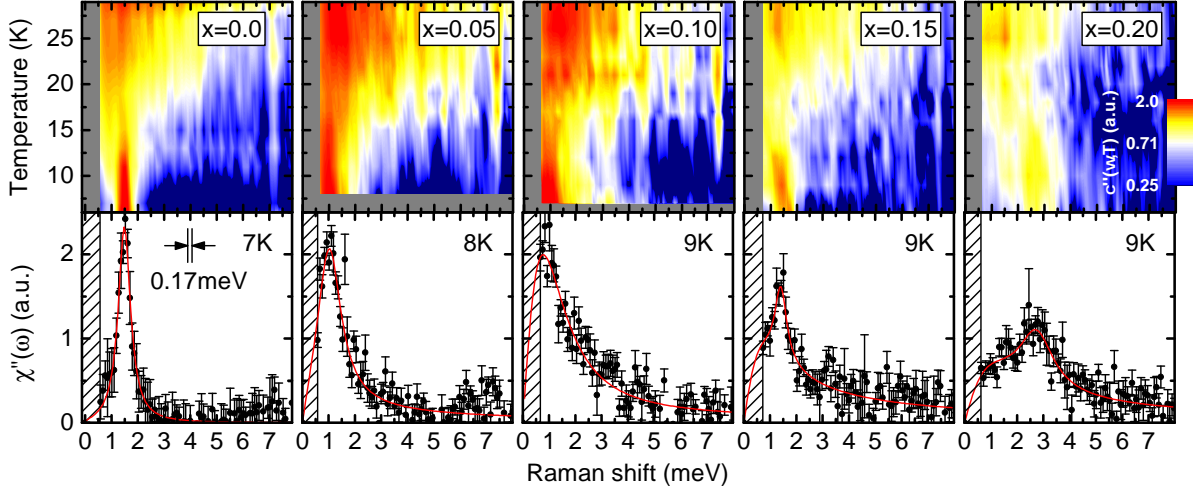


FIG. 2. Low temperature Raman response in the  $A_{2g}$  symmetry channel,  $\chi''_{A_{2g}}(\omega, T)$  [28]. The upper panels show intensity plots, where the intensities are color coded in logarithmic scale. The lower panels show the spectra at about half the transition temperature to emphasize the collective mode, where the error bars represent one standard deviation, and the red solid lines are guides to the eye. The energies of this mode as function of the Fe concentration  $x$  are shown in Fig. 1(a).

two low-lying singlet orbital levels on uranium sites as suggested by recent experiment [33], separated by small energy  $\omega_0$ . These states with pseudovector-like  $A_{2g}$  and full-symmetric  $A_{1g}$  symmetries are denoted by  $|A_{2g}\rangle$  and  $|A_{1g}\rangle$ , respectively. At high temperatures, the crystal field states are quasidegenerate in energy and localized at the uranium  $f$  shells in space. The Curie-Weiss-like behavior above 100 K in static magnetic- [3, 34] and Raman-susceptibilities [17, 35, 36] suggest  $A_{2g}$  pseudovector-like instabilities at low temperature. Below about 50 K, the Kondo screening begins setting in [16, 30, 32, 34, 37] and the correlation length of the HO [38] or LMAF [4, 39] phase builds at the ordering vector  $Q_0 = (0, 0, 1)$ ; therefore both the magnetic and Raman uniform susceptibilities start to decrease [Fig. 3]. Close to the transition temperature, both the HO and LMAF order parameters fluctuate regardless of the low temperature ordering [Figs. 1(b)–1(d)]. However, the static magnetic susceptibility at  $Q_0$  diverges only across the PM–LMAF phase transition [4, 18], whereas it becomes “near critical” from the PM–HO phase [38]. Thus, HO is a nonmagnetic transition, but there is the “ghost” of LMAF present as shown in Fig. 1(b). Here, we find that the temperature dependencies of the static  $A_{2g}$  Raman susceptibility  $\chi_{A_{2g}}(0, T)$  are similar and track  $\chi_c^m(T)$  in all measured samples, suggesting that the minimal model is applicable for the studied Fe substituted crystals.

We now discuss the origin and the observed doping dependence of the collective mode in the ordered phases within a phenomenological Ginzburg-Landau approach. Within the minimal model, the two order parameters can be constructed from  $|A_{2g}\rangle$  and  $|A_{1g}\rangle$  [19]. The HO phase was explained as the state in which the two levels mix, resulting in a lower symmetry point group on

the uranium site, which breaks all vertical and diagonal reflection symmetry planes, and thus acquires left and right handedness. [17, 19] The staggering of left and right handed solutions on the lattice gives rise to the chirality density wave [17] [Fig. 4(a)]. In the HO phase, the staggered condensate can be approximated by a form  $|\psi_{\text{HO}}\rangle = \prod_{r=A \text{ site}} |\text{HO}_r^+\rangle \times \prod_{r=B \text{ site}} |\text{HO}_r^-\rangle$ . Note that

$|\text{HO}_r^\pm\rangle$  at uranium site  $r$  is dominantly  $|A_{2g}\rangle$ , with a small admixture of  $|A_{1g}\rangle$ , i.e.,  $|\text{HO}^\pm\rangle = \cos\theta |A_{2g}\rangle \pm \sin\theta |A_{1g}\rangle$ .

In the HO phase the orbital mixing is purely real. If, however the mixing is purely imaginary, the charge distribution on the uranium site does not break any spatial symmetry; instead, it acquires nonzero out-of-plane magnetic moments, and thereby breaks time reversal symmetry. The Néel-type condensate [Fig. 4(b)] takes the form  $|\psi_{\text{AF}}\rangle = \prod_{r=A \text{ site}} |\text{AF}_r^+\rangle \times \prod_{r=B \text{ site}} |\text{AF}_r^-\rangle$ , where  $|\text{AF}^\pm\rangle = \cos\theta' |A_{1g}\rangle \pm i \sin\theta' |A_{2g}\rangle$  [19]. The two apparently competing orders, the chirality density wave and the antiferromagnetic state, are both constructed by mixing the two orbital wave functions on uranium sites with a real or an imaginary phase factor,  $\sin\theta$  or  $i \sin\theta'$ , thus unifying the two order parameters.

The Ginzburg-Landau free energy can then be constructed from the two component order parameter  $\Psi^T \equiv (\psi_{\text{HO}} \ \psi_{\text{AF}})$ , where the order parameters correspond to the two condensates  $|\psi_{\text{HO}}\rangle$  and  $|\psi_{\text{AF}}\rangle$  defined above. The free energy takes the form

$$F[\Psi] = \Psi^T \hat{A} \Psi + \beta (\Psi^T \Psi)^2 + \gamma (\Psi^T \hat{\sigma}_1 \Psi)^2 \quad (1)$$

where  $\hat{A} \equiv \begin{pmatrix} \alpha_{\text{HO}} & 0 \\ 0 & \alpha_{\text{AF}} \end{pmatrix}$ , with  $\alpha_{\text{HO}}$  and  $\alpha_{\text{AF}}$  vanish at

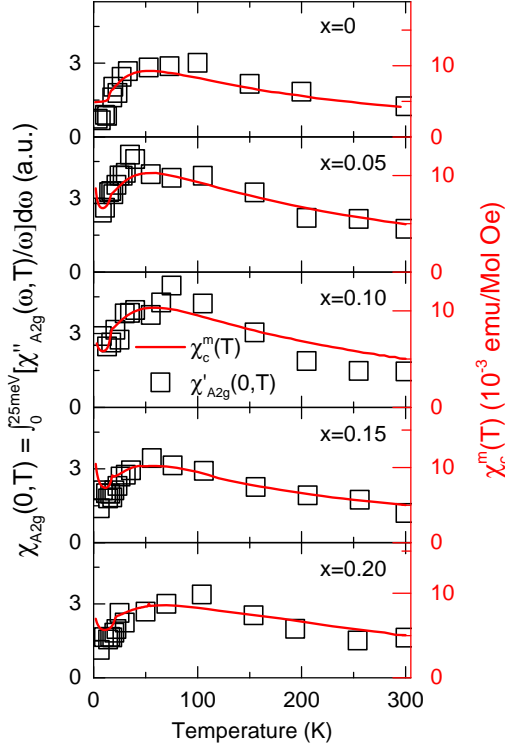


FIG. 3. The static Raman susceptibility in the  $A_{2g}$  symmetry channel (open squares)  $\chi_{A_{2g}}(0, T)$ , compared with the magnetic susceptibility with field applied along the  $c$  axis [3] (solid line).

the critical temperature.  $\hat{\sigma}_1 \equiv \begin{pmatrix} 0 & 1 \\ 1 & 0 \end{pmatrix}$  is the Pauli matrix.  $\gamma$  controls a finite barrier between the two minima in Figs. 1(e)–1(g), and hence ensures phase separation between the HO and LMAF phases [39]. The free energy parameters are introduced following the recipes given in Haule and Kotliar [20, 40] with adjustments to match the phase diagram in Fig. 1(a) [28].

The Ginzburg-Landau free energy in the two dimensional space of  $\psi_{\text{HO}}$  and  $\psi_{\text{AF}}$  is shown in Figs. 1(b)–1(g). Below the second order phase transition, two global and two local minima develop on  $\psi_{\text{HO}}$  and  $\psi_{\text{AF}}$  axes due to spontaneous discrete symmetry breaking, where the minima characterize the ground states in the HO and LMAF phases, respectively.

At the critical doping [Fig. 1(f)], the four minima are degenerate, but the barrier between the minima remains finite due to a  $\gamma$  term in Ginzburg-Landau functional. Therefore the transition between HO and LMAF phases is of the first order, and the coexistence of both phases is allowed, explaining the LMAF puddles that have been observed in the HO phase [41, 42].

The energy separation between the dominant long range order (e.g.,  $|\psi_{\text{HO}}\rangle$ ) and the sub-dominant order (e.g.,  $|\psi_{\text{AF}}\rangle$ ) is vanishingly small at the critical Fe con-

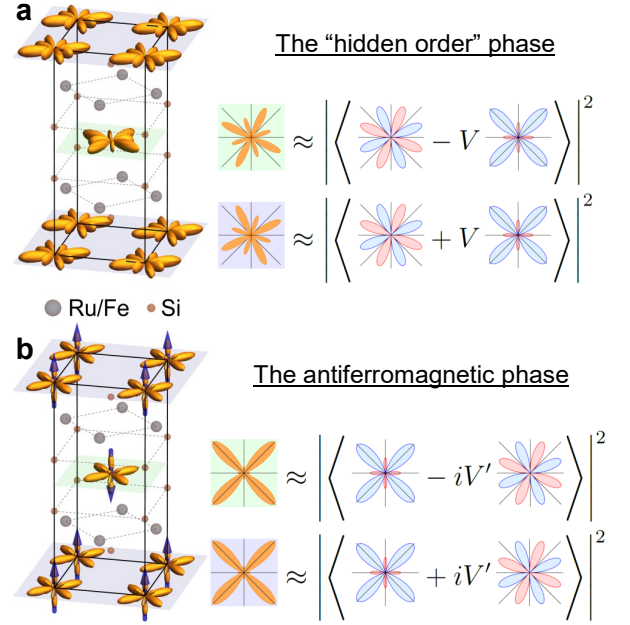


FIG. 4. The crystal structure of  $\text{URu}_{2-x}\text{Fe}_x\text{Si}_2$  in (a) the HO and (b) the LMAF phases. Illustrations capturing the symmetries of the charge distributions of the ground state wave functions are placed at the uranium atomic sites. On the right are illustrations showing the in-plane structures of the wave functions. In the HO phase, the crystal field state with the lowest energy has  $A_{2g}$  symmetry with 8 nodal lines,  $|A_{2g}\rangle$ , which mixes with the first excited state with  $A_{1g}$  symmetry,  $|A_{1g}\rangle$ , to form the local wave functions in the HO phase,  $|\text{HO}^\pm\rangle \approx \cos \theta |A_{2g}\rangle \pm \sin \theta |A_{1g}\rangle$ . In the LMAF phase, the ordering of the crystal field states switches, and the new wave functions in the LMAF phase are,  $|\text{AF}^\pm\rangle \approx \cos \theta' |A_{1g}\rangle \pm i \sin \theta' |A_{2g}\rangle$ . Here,  $\theta \equiv \arcsin(V/\omega_0)$  and  $\theta' \equiv \arcsin(V'/\omega_0)$ , respectively.  $\omega_0$  is the splitting between the lowest lying crystal field states in the minimal model.  $V$  and  $V'$  are the order parameter strength in the HO and LMAF phases, respectively.

centration, and even away from this point can be smaller than the size of the gap. The exciton of subdominant symmetry (e.g.,  $|\psi_{\text{AF}}\rangle$ ) can form in the gap, which then propagates through the order of the dominant symmetry (e.g.,  $|\psi_{\text{HO}}\rangle$ ). Likewise, when the ground state is of  $|\psi_{\text{AF}}\rangle$ , the propagating exciton is of  $|\psi_{\text{HO}}\rangle$  symmetry. The symmetry difference between the two condensates is  $A_{2g}$ ; hence, such exciton can be detected by Raman in the  $A_{2g}$  channel, and explains the sharp resonance shown in Fig. 2. It is clear from this discussion that the energy of the resonance vanishes at the critical Fe concentration, and is linearly increasing away from the critical point. For superconductors, such an excitation is known as the Bardasis-Schrieffer mode, characterizing the transition between two competing Cooper pairing channels [43].

More generally, the uranium-5f orbitals in solids can arrange in surprising types of orders, including orders with broken chirality or time reversal symmetry. While



such orders are competing for the same phase space in  $\text{URu}_2\text{Si}_2$ , they are also subtly connected and were here unified into a common order parameter, which can be switched with small energy cost. The low energy excitations are usually Goldstone modes, but here we detected a new type of excitation, which connects two types of long range order, and is observed as a resonance by light scattering. The resonance brings light to a long-standing problem of emergent phases of exotic local orbital self-organization and their interrelation.

We are grateful for discussions with C. Broholm, N.P. Butch, P. Coleman, I.R. Fisher, P.B. Wiegmann and V.M. Yakovenko. G.B. and H.-H.K. acknowledge support from DOE BES Grant No. DE-SC0005463. A.L. and V.K. acknowledge NSF Grant No. DMR-1104884. K.H. acknowledges NSF Grant No. DMR-1405303. M.B.M., S.R., and N.K. acknowledge DOE BES Grant No. DE-FG02-04ER46105 (crystal growth) and NSF Grant No. DMR-1206553 (materials characterization).

---

\* [hk458@physics.rutgers.edu](mailto:hk458@physics.rutgers.edu)

† [girsh@physics.rutgers.edu](mailto:girsh@physics.rutgers.edu)

- [1] Jesse S. Hall, M. Rahimi Movassagh, M. N. Wilson, G. M. Luke, N. Kanchanavatee, K. Huang, M. Janoschek, M. B. Maple, and T. Timusk, “Electrodynamics of the antiferromagnetic phase in  $\text{URu}_2\text{Si}_2$ ,” *Phys. Rev. B* **92**, 195111 (2015).
- [2] N. Kanchanavatee, M. Janoschek, R. E. Baumbach, J. J. Hamlin, D. A. Zocco, K. Huang, and M. B. Maple, “Twofold enhancement of the hidden-order/large-moment antiferromagnetic phase boundary in the  $\text{URu}_{2-x}\text{Fe}_x\text{Si}_2$  system,” *Phys. Rev. B* **84**, 245122 (2011).
- [3] Sheng Ran, Christian T. Wolowiec, Inho Jeon, Naveen Pouse, Noravee Kanchanavatee, Benjamin D. White, Kevin Huang, Dinesh Martien, Tyler DaPron, David Snow, Mark Williamsen, Stefano Spagna, Peter S. Riseborough, and M. Brian Maple, “Phase diagram and thermal expansion measurements on the system  $\text{URu}_{2x}\text{Fe}_x\text{Si}_2$ ,” *Proc. Natl. Acad. Sci. U.S.A.* **113**, 13348–13353 (2016).
- [4] Nicholas P. Butch, Jason R. Jeffries, Songxue Chi, Juscelino Batista Leão, Jeffrey W. Lynn, and M. Brian Maple, “Antiferromagnetic critical pressure in  $\text{URu}_2\text{Si}_2$  under hydrostatic conditions,” *Phys. Rev. B* **82**, 060408 (2010).
- [5] Frederic Bourdarot, Nicolas Martin, Stephane Raymond, Louis-Pierre Regnault, Dai Aoki, Valentin Taufour, and Jacques Flouquet, “Magnetic properties of  $\text{URu}_2\text{Si}_2$  under uniaxial stress by neutron scattering,” *Phys. Rev. B* **84**, 184430 (2011).
- [6] M. Jaime, K. H. Kim, G. Jorge, S. McCall, and J. A. Mydosh, “High magnetic field studies of the hidden order transition in  $\text{URu}_2\text{Si}_2$ ,” *Phys. Rev. Lett.* **89**, 287201 (2002).
- [7] Dai Aoki, Frédéric Bourdarot, Elena Hassinger, Georg Knebel, Atsushi Miyake, Stéphane Raymond, Valentin Taufour, and Jacques Flouquet, “Field Reentrance of the Hidden Order State of  $\text{URu}_2\text{Si}_2$  under Pressure,” *J. Phys. Soc. Jpn.* **78**, 053701 (2009).
- [8] T. T. M. Palstra, A. A. Menovsky, J. van den Berg, A. J. Dirkmaat, P. H. Kes, G. J. Nieuwenhuys, and J. A. Mydosh, “Superconducting and magnetic transitions in the heavy-fermion system  $\text{URu}_2\text{Si}_2$ ,” *Phys. Rev. Lett.* **55**, 2727–2730 (1985).
- [9] M. B. Maple, J. W. Chen, Y. Dalichaouch, T. Kohara, C. Rossel, M. S. Torikachvili, M. W. McElfresh, and J. D. Thompson, “Partially gapped Fermi surface in the heavy-electron superconductor  $\text{URu}_2\text{Si}_2$ ,” *Phys. Rev. Lett.* **56**, 185–188 (1986).
- [10] W. Schlabbitz, J. Baumann, B. Pollit, U. Rauchschwalbe, H.M. Mayer, U. Ahlheim, and C.D. Bredl, “Superconductivity and Magnetic Order in a Strongly Interacting Fermi-System:  $\text{URu}_2\text{Si}_2$ ,” *Z. Phys. B* **62**, 171–177 (1986).
- [11] E. R. Schemm, R. E. Baumbach, P. H. Tobash, F. Ronning, E. D. Bauer, and A. Kapitulnik, “Evidence for broken time-reversal symmetry in the superconducting phase of  $\text{URu}_2\text{Si}_2$ ,” *Phys. Rev. B* **91**, 140506 (2015).
- [12] Pegor Aynajian, Eduardo H da Silva Neto, Colin V Parker, Yingkai Huang, Abhay Pasupathy, John Mydosh, and Ali Yazdani, “Visualizing the formation of the Kondo lattice and the hidden order in  $\text{URu}_2\text{Si}_2$ ,” *Proc. Natl. Acad. Sci. U.S.A.* **107**, 10383–8 (2010).
- [13] A R Schmidt, M H Hamidian, P Wahl, F Meier, A V Balatsky, J D Garrett, T J Williams, G M Luke, and J C Davis, “Imaging the Fano lattice to ‘hidden order’ transition in  $\text{URu}_2\text{Si}_2$ ,” *Nature (London)* **465**, 570–6 (2010).
- [14] R Okazaki, T Shibauchi, HJ Shi, Y Haga, TD Matsuda, E Yamamoto, Y Onuki, H Ikeda, and Y Matsuda, “Rotational symmetry breaking in the hidden-order phase of  $\text{URu}_2\text{Si}_2$ ,” *Science* **331**, 439–42 (2011).
- [15] Scott C. Riggs, M. C. Shapiro, Akash V. Maharaj, S. Raghu, E. D. Bauer, R. E. Baumbach, P. Giraldo-Gallo, Mark Wartenbe, and I. R. Fisher, “Evidence for a nematic component to the hidden-order parameter in  $\text{URu}_2\text{Si}_2$  from differential elastoresistance measurements,” *Nat. Commun.* **6** (2015).
- [16] J. A. Mydosh and P. M. Oppeneer, “Colloquium: Hidden order, superconductivity, and magnetism: The unsolved case of  $\text{URu}_2\text{Si}_2$ ,” *Rev. Mod. Phys.* **83**, 1301–1322 (2011), and references therein.
- [17] H.-H. Kung, R. E. Baumbach, E. D. Bauer, V. K. Thorsmølle, W.-L. Zhang, K. Haule, J. A. Mydosh, and G. Blumberg, “Chirality density wave of the ‘hidden order’ phase in  $\text{URu}_2\text{Si}_2$ ,” *Science* **347**, 1339–1342 (2015).
- [18] Pinaki Das, N. Kanchanavatee, J. S. Helton, K. Huang, R. E. Baumbach, E. D. Bauer, B. D. White, V. W. Burnett, M. B. Maple, J. W. Lynn, and M. Janoschek, “Chemical pressure tuning of  $\text{URu}_2\text{Si}_2$  via isoelectronic substitution of Ru with Fe,” *Phys. Rev. B* **91**, 085122 (2015).
- [19] Kristjan Haule and Gabriel Kotliar, “Arrested Kondo effect and hidden order in  $\text{URu}_2\text{Si}_2$ ,” *Nat. Phys.* **5**, 796–799 (2009).
- [20] K. Haule and G. Kotliar, “Complex Landau-Ginzburg theory of the hidden order in  $\text{URu}_2\text{Si}_2$ ,” *Europhys. Lett.* **89**, 57006 (2010).
- [21] Y. J. Jo, L. Balicas, C. Capan, K. Behnia, P. Lejay, J. Flouquet, J. A. Mydosh, and P. Schlottmann, “Field-induced fermi surface reconstruction and adiabatic continuity between antiferromagnetism and the hidden-order state in  $\text{URu}_2\text{Si}_2$ ,” *Phys. Rev. Lett.* **98**, 166404 (2007).
- [22] E. Hassinger, G. Knebel, K. Izawa, P. Lejay, B. Salce,

- and J. Flouquet, “Temperature-pressure phase diagram of  $\text{URu}_2\text{Si}_2$  from resistivity measurements and ac calorimetry: Hidden order and fermi-surface nesting,” *Phys. Rev. B* **77**, 115117 (2008).
- [23] C. Broholm, J. K. Kjems, W. J. L. Buyers, P. Matthews, T. T. M. Palstra, A. A. Menovsky, and J. A. Mydosh, “Magnetic excitations and ordering in the heavy-electron superconductor  $\text{URu}_2\text{Si}_2$ ,” *Phys. Rev. Lett.* **58**, 1467–1470 (1987).
- [24] T. J. Williams, H. Barath, Z. Yamani, J. A. Rodriguez-Riviera, J. B. Leão, J. D. Garrett, G. M. Luke, W. J. L. Buyers, and C. Broholm, “Gapped excitations in the high-pressure antiferromagnetic phase of  $\text{URu}_2\text{Si}_2$ ,” (2016), [arXiv:1607.00967 \[cond-mat.str-el\]](#).
- [25] M. N. Wilson, T. J. Williams, Y.-P. Cai, A. M. Hallas, T. Medina, T. J. Munsie, S. C. Cheung, B. A. Frandsen, L. Liu, Y. J. Uemura, and G. M. Luke, “Antiferromagnetism and hidden order in isoelectronic doping of  $\text{URu}_2\text{Si}_2$ ,” *Phys. Rev. B* **93**, 064402 (2016).
- [26] Nicholas P. Butch, Sheng Ran, Inho Jeon, Noravee Kanchanavatee, Kevin Huang, Alexander Breindel, M. Brian Maple, Ryan L. Stillwell, Yang Zhao, Leland Harriger, and Jeffrey W. Lynn, “Distinct magnetic spectra in the hidden order and antiferromagnetic phases in  $\text{URu}_{2-x}\text{Fe}_x\text{Si}_2$ ,” *Phys. Rev. B* **94**, 201102 (2016).
- [27] T. J. Williams, M. N. Wilson, A. A. Aczel, M. B. Stone, and G. M. Luke, “Hidden Order Signatures in the Antiferromagnetic Phase of  $\text{U}(\text{Ru}_{1-x}\text{Fe}_x)_2\text{Si}_2$ ,” (2016), [arXiv:1607.05672 \[cond-mat.str-el\]](#).
- [28] See Supplemental Material at [URL will be inserted by publisher] for details of material growth and data analysis.
- [29] D. V. Khveshchenko and P. B. Wiegmann, “Raman scattering and anomalous current algebra in mott insulators,” *Phys. Rev. Lett.* **73**, 500–503 (1994).
- [30] W. T. Guo, Z. G. Chen, T. J. Williams, J. D. Garrett, G. M. Luke, and N. L. Wang, “Hybridization gap versus hidden-order gap in  $\text{URu}_2\text{Si}_2$  as revealed by optical spectroscopy,” *Phys. Rev. B* **85**, 195105 (2012).
- [31] R. P. S. M. Lobo, J. Buhot, M. A. Méasson, D. Aoki, G. Lapertot, P. Lejay, and C. C. Homes, “Optical conductivity of  $\text{URu}_2\text{Si}_2$  in the kondo liquid and hidden-order phases,” *Phys. Rev. B* **92**, 045129 (2015).
- [32] Jesse S. Hall, Urmas Nagel, Taaniel Uleksin, Toomas Rõõm, Travis Williams, Graeme Luke, and Thomas Timusk, “Observation of multiple-gap structure in hidden order state of  $\text{URu}_2\text{Si}_2$  from optical conductivity,” *Phys. Rev. B* **86**, 035132 (2012).
- [33] Martin Sundermann, Maurits W Haverkort, Stefano Agrestini, Ali Al-Zein, Marco Moretti Sala, Yingkai Huang, Marc Golden, Anne de Visser, Peter Thalmeier, Liu Hao Tjeng, and Andrea Severing, “Direct bulk sensitive probe of 5f symmetry in  $\text{URu}_2\text{Si}_2$ ,” (2016), [arXiv:1608.01840 \[cond-mat.str-el\]](#).
- [34] C. Pfleiderer, J. A. Mydosh, and M. Vojta, “Pressure dependence of the magnetization of  $\text{URu}_2\text{Si}_2$ ,” *Phys. Rev. B* **74**, 104412 (2006).
- [35] S. L. Cooper, M. V. Klein, M. B. Maple, and M. S. Torikachvili, “Magnetic excitations and phonon anomalies in  $\text{URu}_2\text{Si}_2$ ,” *Phys. Rev. B* **36**, 5743–5746 (1987).
- [36] J. Buhot, M.-A. Méasson, Y. Gallais, M. Cazayous, A. Sacuto, G. Lapertot, and D. Aoki, “Symmetry of the excitations in the hidden order state of  $\text{URu}_2\text{Si}_2$ ,” *Phys. Rev. Lett.* **113**, 266405 (2014).
- [37] J. Levallois, F. Lévy-Bertrand, M. K. Tran, D. Stricker, J. A. Mydosh, Y.-K. Huang, and D. van der Marel, “Hybridization gap and anisotropic far-infrared optical conductivity of  $\text{URu}_2\text{Si}_2$ ,” *Phys. Rev. B* **84**, 184420 (2011).
- [38] P. G. Niklowitz, S. R. Dunsiger, C. Pfleiderer, P. Link, A. Schneidewind, E. Faulhaber, M. Vojta, Y.-K. Huang, and J. A. Mydosh, “Role of commensurate and incommensurate low-energy excitations in the paramagnetic to hidden-order transition of  $\text{URu}_2\text{Si}_2$ ,” *Phys. Rev. B* **92**, 115116 (2015).
- [39] P. G. Niklowitz, C. Pfleiderer, T. Keller, M. Vojta, Y.-K. Huang, and J. A. Mydosh, “Parasitic Small-Moment Antiferromagnetism and Nonlinear Coupling of Hidden Order and Antiferromagnetism in  $\text{URu}_2\text{Si}_2$  Observed by Larmor Diffraction,” *Phys. Rev. Lett.* **104**, 106406 (2010).
- [40] Lance Boyer and Victor Yakovenko, “A model for the polar kerr effect in the hidden-order phase of  $\text{URu}_{2-x}\text{Fe}_x\text{Si}_2$ ,” *APS March Meeting Baltimore Abstracts* **R22**, 4 (2016).
- [41] K. Matsuda, Y. Kohori, T. Kohara, K. Kuwahara, and H. Amitsuka, “Spatially inhomogeneous development of antiferromagnetism in  $\text{URu}_2\text{Si}_2$ : Evidence from  $^{29}\text{Si}$  NMR under pressure,” *Phys. Rev. Lett.* **87**, 087203 (2001).
- [42] M. Yokoyama, H. Amitsuka, K. Tenya, K. Watanabe, S. Kawarazaki, H. Yoshizawa, and J. A. Mydosh, “Competition between hidden order and antiferromagnetism in  $\text{URu}_2\text{Si}_2$  under uniaxial stress studied by neutron scattering,” *Phys. Rev. B* **72**, 214419 (2005).
- [43] A. Bardasis and J. R. Schrieffer, “Excitons and plasmons in superconductors,” *Phys. Rev.* **121**, 1050–1062 (1961).